2009 International Symposium on Nonlinear Theory and its Applications
NOLTA'09, Sapporo, Japan, October 18-21, 2009

A Simple Switched Dynamical System based on Photovoltaic Systems

Daisuke Kimura† and Toshimichi Saito†

†EE Dept., Hosei University, Koganei, Tokyo, 184-0002 Japan; tsaito AT hosei.ac.jp

Abstract—This paper studies a piecewise linear switched dynamical system based on the photovoltaic systems. The input is represented by a current-controlled voltage source and is converted to the output through a circuit whose switching depends on both time and state variable. Applying the mapping procedure, we have analyzed basic bifurcation of fixed points which correspond to desired operation of the photovoltaic systems. Especially, we have found two interesting phenomena. (1) Two stable fixed points can co-exist and the system exhibits either one depending on the initial state. (2) The maximum power point is given for an unstable fixed point. These results provide basic information for design of reliable and stable systems.

1. Introduction

This paper studies dynamics of a simple switched dynamical system (SDS) based on the photovoltaic systems [1]-[9]. The SDS is characterized by nonlinear switching among several sub-dynamics and has been studied extensively [10]-[12]. The SDS relates to many important engineering systems (e.g., power converters and analog-to-digital converters) and its analysis can provide basic information to design efficient systems. The nonlinear switching can cause interesting bifurcation phenomena and its analysis is an important nonlinear problem.

This paper presents a piecewise linear SDS relating to the photovoltaic systems and the maximum power point trackers (MPPT). In the SDS, the input is represented by a current-controlled voltage source (CCVS) having piecewise linear characteristic that can be regarded as a simplified model of the solar cells [1] [2]. The Input is converted to the output through a circuit consisting of one inductor, one diode and one switch. The switching depends on both periodic clock signal and inductor current; and can cause rich periodic/chaotic phenomena. Applying simplification technique in our previous works [12]-[14], essential system parameters are extracted and the SDS dynamics is simplified into the phase map that is a one-dimensional difference equation for the switching phase. Using the piecewise exact solution, the phase map can be described exactly and precise analysis is possible. Using the phase map, we have analyzed bifurcation of fixed points which correspond to desired operation of the photovoltaic systems. Especially, we have found two interesting phenomena in some parameter subspace. First, two stable fixed points can co-exist and the SDS exhibits either one depending on initial state: special attention should be paid to initial state in order to realize stable operation. Such co-existing fixed points are impossible in the SDS based on dc-dc converters [14]. Second, the maximum power point is given for an unstable fixed point: stabilizing the fixed point is important to realize efficient MPPT [15]. That is, our results provide basic information for design of reliable and stable systems.

The MPPT is an important technique in renewable energy problems and various control methods have been studied [3, 4, 6, 7]. However, global stability has not been analyzed sufficiently, so far. The small signal analysis for local stability has been mainstream in existing works on MPPT [4, 8]. Our phase map is derived from a simplified system, however, can clarify global stability and chaos, precisely.

2. The Circuit Model

Fig. 1 shows a circuit model of the SDS where the CCVS has two-segment piecewise linear characteristics.

$$V_i(i) = \begin{cases} -a(i - I_p) + V_p & \text{for } i \le I_p \\ -b(i - I_p) + V_p & \text{for } i > I_p \end{cases} \quad (1)$$

where $i \ge 0$ and $V_i(i) \ge 0$ are assumed. This CCVS can be regarded as a simplified model of solar cells [1] [3]. Although the solar cells are usually described by a voltage-controlled function, the function is one-to-one and the current-controlled description is convenient to derive circuit equation for inductor current. It goes without saying that real solar cell parameters vary depending on insolation, however, we will fix the parameters in this paper. The circuit has a switch S and a diode D which can be either of the two states.

State 1: S conducting and D blocking
State 2: S blocking and D conducting

The switching rule is defined by

State 1 → State 2: when $i = J_u$
State 2 → State 1: when $t = nT$ or $i = J_l$.

where J_u and J_l are upper and lower thresholds, respectively. T is a clock period as shown in Fig. 1. Note that the lower threshold $J_l \ge 0$ prohibits discontinuous conduction mode where both S and D are blocking. For simplicity, we assume that the time constant of the load is much larger than the clock period ($RC >> T$). In this case the output load can be replaced with the constant voltage source [12] - [14] and the circuit dynamics is described by

$$L\frac{di}{dt} = \begin{cases} V_i(i) & \text{for State 1} \\ V_i(i) - V_o & \text{for State 2} \end{cases} \quad (2)$$

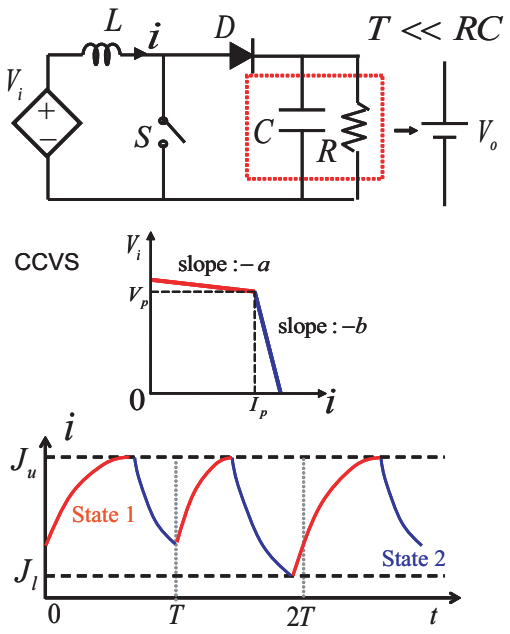

Figure 1: Circuit model and switching rule.

where we assume the boost operation: $V_o > V_i(i)$ for $i \geq 0$ (or $V_o > V_p + aI_p$). We have also assumed that all the circuit elements are ideal and the switching is instantaneous [12]. Using the dimensionless variables and parameters:

$$\tau = \frac{t}{T},\ x = \frac{i}{I_p},\ y(x) = \frac{V_i(I_p x)}{V_p},\ \alpha = \frac{aI_p}{V_p},\ \beta = \frac{bI_p}{V_p}$$
$$\gamma = \frac{TV_p}{LI_p},\ q = \frac{V_o}{V_p},\ X_+ = \frac{J_u}{I_p},\ X_- = \frac{J_l}{I_p}, \tag{3}$$

Equation (2) and the switching rule are transformed into

$$\frac{dx}{d\tau} = \begin{cases} \gamma y(x) & \text{for State 1} \\ \gamma(y(x) - q) & \text{for State 2} \end{cases}$$
$$y(x) = \begin{cases} -\alpha(x-1)+1 & \text{for } x \leq 1 \\ -\beta(x-1)+1 & \text{for } x > 1 \end{cases} \tag{4}$$

State 1 → State 2: when $x = X_+$
State 2 → State 1: when $\tau = n$ or $x = X_-$.

The piecewise exact solution for initial condition $(\tau, x) = (\tau_0, x_0)$ is given by

State 1:
$$x(\tau) = (x_0 - x_{e1})e^{-\gamma\alpha(\tau-\tau_0)} + x_{e_1} \quad \text{for } x \leq 1$$
$$x(\tau) = (x_0 - x_{e2})e^{-\gamma\beta(\tau-\tau_0)} + x_{e_2} \quad \text{for } x > 1$$

State 2:
$$x(\tau) = (x_0 + x_{e3})e^{-\gamma\alpha(\tau-\tau_0)} - x_{e_3} \quad \text{for } x \leq 1$$
$$x(\tau) = (x_0 + x_{e4})e^{-\gamma\beta(\tau-\tau_0)} - x_{e_4} \quad \text{for } x > 1 \tag{5}$$

where $x_{e1} = 1 + 1/\alpha$, $x_{e2} = 1 + 1/\beta$, $x_{e3} = q/\alpha - 1 - 1/\alpha$ and $x_{e4} = q/\beta - 1 - 1/\beta$. The condition $V_o > V_p + aI_p$ guarantees $x_{e3} > 0$ and $x_{e4} > 0$. Using these, the orbits can be calculated precisely.

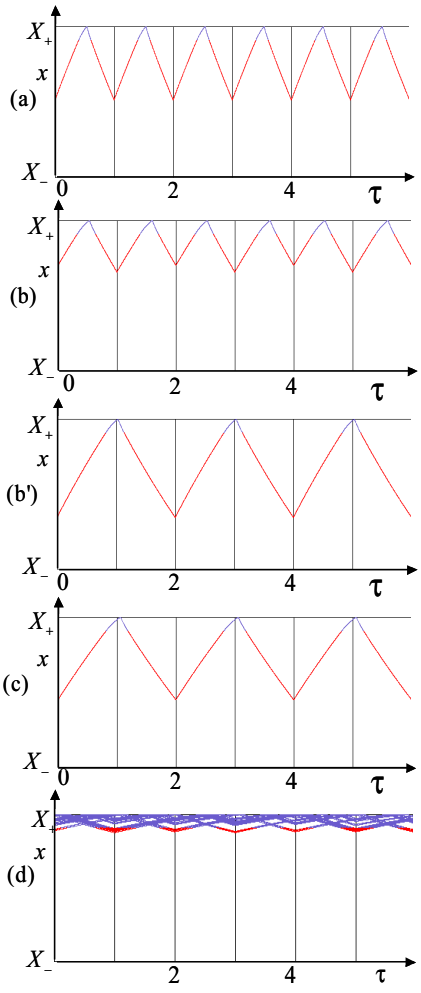

Figure 2: Typical Waveforms for $\alpha = 0.4$, $\beta = 5$, $X_+ = 1.1$, $X_- = 0$ and $q = 2.2$. (a) Periodic orbit for $\gamma = 1$, (b) and (b') Co-existing periodic orbits for $\gamma = 0.67$, (c) Periodic orbit for $\gamma = 0.56$. (d) Chaotic orbit for $\gamma = 0.1$

The dimensionless six parameters can be classified into two categories: (α, β, q) can represent "solar cell and load" characteristics and (γ, X_+, X_-) can represent "control" in the boost converter. The problem is to consider roles of (γ, X_+, X_-) in the circuit performance for variation of (α, β, q). However, consideration for all the parameters is hard in this paper. For simplicity, we focus on the parameter $\gamma \equiv \frac{TV_p}{LI_p}$ and fix the other parameters by trial-and-errors. Also, we assume that I_p and V_p are fixed. We then define the dimensionless instantaneous power by $p(\tau) = x(\tau)y(\tau)$.

Fig. 2 shows typical orbits. The circuit has unique periodic orbit in (a) for $\gamma = 1$. As γ decreases (T decreases), the behavior is changed into co-existing stable orbits in (b) and (b') where the circuit exhibits either depending on the initial states. The behavior is then changed into a unique periodic orbit in (c) and into chaotic orbit in (d).

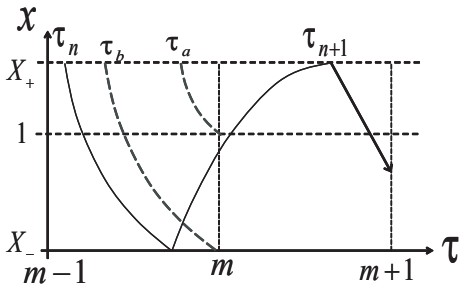

Figure 3: Definition of switching time.

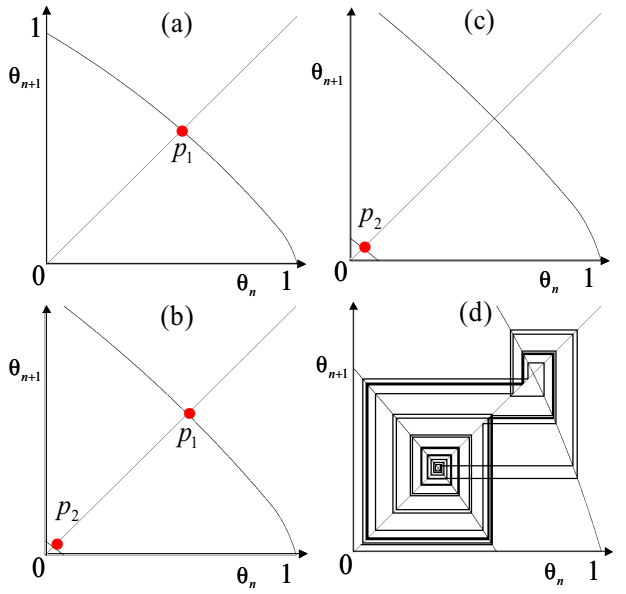

Figure 4: Phase maps for $\alpha = 0.4$, $\beta = 5$, $X_+ = 1.1$, $X_- = 0$ and $q = 2.2$. (a) Stable fixed point p_1 for $\gamma = 1$, (b) Co-existing stable fixed points p_1 and p_2 for $\gamma = 0.67$, (c) Stable fixed point p_2 for $\gamma = 0.56$, (d) Chaos for $\gamma = 0.1$.

3. Phase map and Analysis

In order to analyze the dynamics precisely, we define the phase map. As shown in Fig. 3, let τ_n denote the n-th switching time at the upper threshold X_+. Since τ_n determines τ_{n+1}, we can define a one dimensional map F from positive reals $\boldsymbol{R}^+$ to itself. Its iteration can represent the circuit dynamics:

$$\tau_{n+1} = \begin{cases} \frac{1}{\beta\gamma}\ln(k_1 e^{(-\gamma\beta(\tau_n-1))} - \frac{q}{\beta}) + k_2 & \text{for } \tau_a < \tau_n \le 1 \\ \frac{1}{\alpha\gamma}\ln(k_3 e^{(-\gamma\alpha(\tau_n-1))} + q) + k_4 & \text{for } \tau_b < \tau_n \le \tau_a \\ \tau_1 + k_5 & \text{for } 0 < \tau_n \le \tau_b \end{cases} \tag{6}$$

Where $\tau_a = \frac{1}{\beta\gamma}\ln(\frac{q-1}{(\beta X_+ - 1 - \beta + q)})$, $\tau_b = \tau_a + \frac{1}{\gamma\alpha}\ln(\frac{q-1-\alpha}{q-1}) + 1$, $k_1 = X_+ - 1 - \frac{1}{\beta} + \frac{q}{\beta}$, $k_2 = -\ln(k_1 - \frac{q}{\beta}) + 1$, $k_3 = (1-q)(\frac{\beta X_+ - \beta}{q-1} + 1)^{\frac{\alpha}{\beta}}$, $k_4 = \frac{1}{\beta\gamma}\ln(\frac{1}{1+\beta-\beta X_+}) + 1$, $k_5 = k_4 + \frac{1}{\beta\gamma}\ln(\frac{\beta X_+ - 1}{q-1} + 1) + \frac{1}{\gamma\alpha}\ln(\frac{(1+\alpha)(q-1)}{q-1-\alpha}) - 1$. Using the exact piecewise solution in (5), the map can be calculated exactly. For convenience, we introduce a phase variable $\theta_n = \tau_n \bmod 1$. Using this, the map F can be simplified into the phase map f from unit interval $I \equiv [0, 1)$ to itself:

$$\theta_{n+1} = f(\tau_n) = F(\theta_n) \bmod 1, \quad \theta_n \in I \tag{7}$$

That is, the circuit dynamics can be integrated into the iteration of this phase map.

Fig. 4 shows typical shapes of the phase map for the same parameter values as Fig. 2. The stable fixed point p_1 in (a) corresponds to periodic orbit in Fig. 2 (a). As

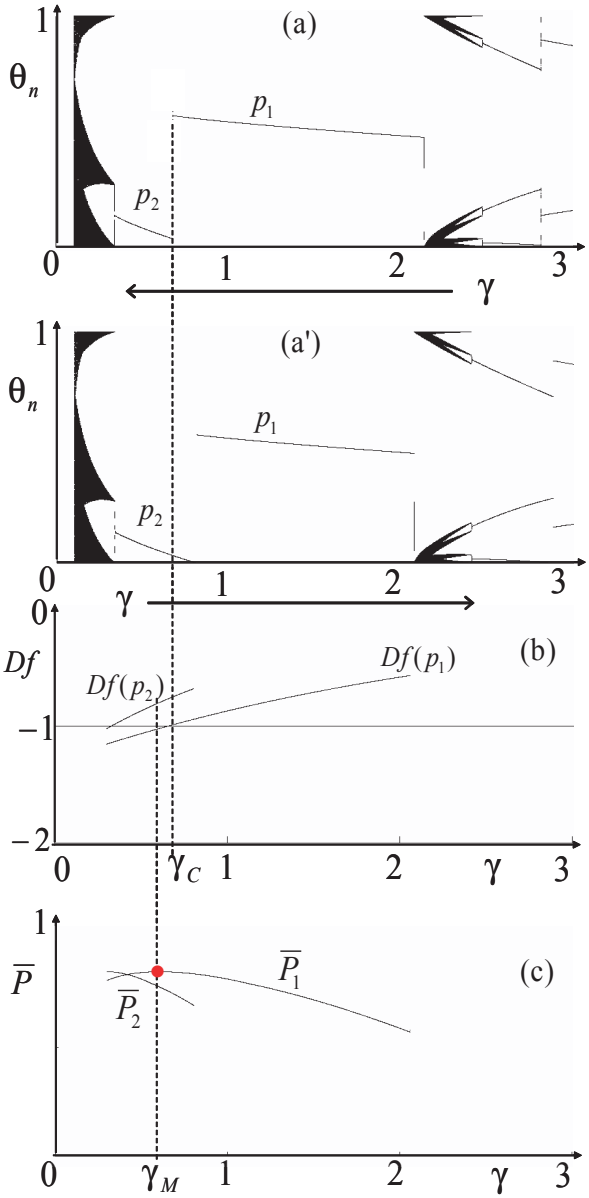

Figure 5: Bifurcation for $\alpha = 0.4$, $\beta = 5$, $X_+ = 1.1$, $X_- = 0$ and $q = 2.2$. (a) Attractors of phase map for decreasing γ, (a') That for increasing γ, (b) Slope of fixed point(s), (c) Average power of periodic orbits corresponding to fixed points. $\overline{P}_1$ and $\overline{P}_2$ correspond to p_1 and p_2, respectively. The maximum power point is indicated by the circle.

γ decreases, the second segment appears in the left-side as shown in (b) where the phase map has two stable fixed points p_1 and p_2. The p_1 and p_2 correspond to small and large amplitude orbits in Fig. 2 (b) and (b'), respectively. After that, the fixed point p_1 loses its stability, and the phase map has a unique stable fixed point p_2 in (c). As γ decreases further, the p_2 loses its stability and the phase map exhibits chaotic behavior as shown in (d).

The bifurcation for γ is summarized in Fig. 5 (a) and (a'). The diagram shows various periodic/chaotic attractors and we pay special attention to the fixed points p_1 and p_2. The fixed point corresponds to a desired periodic orbit in the circuit. From MPPT viewpoint, a basic problem is finding parameters that gives the maximum power point for the periodic orbit. Note that Fig. 5 (a) (respectively, (a')) are drawn for decreasing γ (respectively, increasing γ). We can confirm a parameter range on which the fixed point is different: (a) shows p_1, (a') shows p_2 hence they co-exist on this range.

Fig. 5 (b) shows slope of the phase map Df at p_1 and p_2: if the magnitude of the slope is less than one, the phase map is contracting near the fixed point and the fixed point is stable. We can confirm the parameter range (the right side of γ_c) where magnitude of slope is lass than one for both p_1 and p_2: this is the evidence for stability of the co-existing fixed points. The circuit exhibits either fixed point depending on initial state and transition between p_1 and p_2 has hysteresis as suggested in (a) and (a'): the observed phenomenon is switched from p_1 to p_2 as γ decreases, that is switched from p_2 to p_1 as γ increases, and the two thresholds are different. Fig. 5 (c) shows average power $\overline{P}$ of periodic orbits corresponding to the fixed points p_1 and p_2. Note that the maximum power is given at $\gamma = \gamma_M$. Since γ_M is less than γ_C at which p_1 loses its stability, the the maximum power is given on the unstable periodic orbit.

4. Conclusions

The simple piecewise linear circuit model based on photovoltaic systems has been studied in this paper. The circuit includes CCVS that can be regarded as a simplified model of the solar cell. Applying the mapping procedure, basic bifurcation phenomena have been investigated. Especially, we can suggest two important remarks.

- The circuit can have co-existing stable periodic orbits. In the case, we must pay special attention to initial state setting in order to realize suitable circuit operation.
- The unstable periodic orbit (UPO) can give the maximum power point. Stabilizing the objective UPO is important to realize efficient MPPT.

Future problems are many, including detailed analysis of bifurcation phenomena, stabilizing the UPO for design of the MPPT, and design of practical circuits.

References

[1] Y. H. Lim and D. C. Hamill, Chaos in spacecraft power systems. Electron. Lett. 35, 9, pp. 510-511, 1999.

[2] M. Veerachary, T. Senjyu and K. Uezato Neural-Network-Based Maximum-Power-Point Tracking of Coupled-Inductor Interleaved-Boost-Converter-Supplied PV System Using Fuzzy Controller, IEEE Trans. Ind. Electron., 50, 4, pp. 749-758, 2003.

[3] K. K. Tse, B. M. T. Ho, H. S.-H. Chung and S. Y. Ron Hui, A Comparative Study of Maximum-Power-Point Trackers for Photovoltaic Panels Using Switching-Frequency Modulation Scheme, IEEE Trans. Ind. Electron., 51, 2, pp. 410-418, 2004.

[4] K. Kobayashi, H. Matsuo and Y. Sekine, Novel solar-cell power supply system using a multiple-Input dc-dc converter, IEEE Trans. Ind. Electron., 53, 1, pp. 281-286, 2006.

[5] N. Femia, G. Lisi, G. Petrone, G. Spagnuolo and M. Vitelli, Distributed Maximum Power Point Tracking of Photovoltaic Arrays: Novel Approach and System Analysis, IEEE Trans. Ind. Electron., 55, 7, pp. 2610-2621, 2008.

[6] F. Liu, S. Duan, F. Liu, B. Liu and Y. Kang, A Variable Step Size INC MPPT Method for PV Systems, IEEE Trans. Ind. Electron., 55, 7, pp. 2622-2628, 2008.

[7] D. Sera, R. Teodorescu, J. Hantschel and M. Knoll, Optimized Maximum Power Point Tracker for Fast-Changing Environmental Conditions, IEEE Trans. Ind. Electron., 55, 7, pp. 2629-2637, 2008.

[8] N. D. Benavides and P. L. Chapman, Modeling the Effect of Voltage Ripple on the Power Output of Photovoltaic Modules. IEEE Trans. Ind. Electron., 55, 7, pp. 2638-2643, 2008.

[9] R. Gules, J. De Pellegrin Pacheco, H. L. Hey and J. Imhoff, A Maximum Power Point Tracking System With Parallel Connection for PV Stand-Alone Applications, IEEE Trans. Ind. Electron., 55, 7, pp. 2674-2683, 2008.

[10] S. Banerjee and G. C. Verghese, eds., Nonlinear Phenomena in Power Electronics: Attractors, Bifurcations, Chaos, and Nonlinear Control, IEEE Press, 2001.

[11] C. K. Tse and M. di Bernardo, Complex behavior in switching power converters, Proc. IEEE, 90, pp. 768-781, 2002.

[12] T. Saito, T. Kabe, Y. Ishikawa, Y. Matsuoka and H. Torikai, Piecewise constant switched dynamical systems in power electronics, Int'l J. of Bifurcation and Chaos, 17, 10, pp. 3373-3386, 2007.

[13] T. Saito, S. Tasaki and H. Torikai, Interleaved buck converters based on winner-take-all switching, IEEE Trans. Circuits Syst. I, 52, 8, pp. 1666-1672, 2005

[14] D. Kimura and T. Saito, Stability analysis of switched dynamical systems for effective switching strategy of DC/DC converters, Proc. IEEE/IECON, pp. 965-970, 2008.

[15] G. Poddar, K. Chakrabarty and S. Banerjee, Controlling chaos in dc-dc converters, IEEE Trans. Circuits Syst. I, 45, pp. 672 - 676, 1998.